IJE TRANSACTIONS A: Basics Vol. 29, No. 10, (October 2016) 1459-1468

International Journal of Engineering

Journal Homepage: www.ije.ir

Comparison of Properties of Ti/TiN/TiCN/TiAlN Film Deposited by Cathodic Arc Physical Vapor and Plasma-assisted Chemical Vapor Deposition on Custom 450 Steel Substrates

E. Poursaiedi, A. Salarvand*

Department of Mechanical Engineering, University of Zanjan, Zanjan, Iran

PAPER INFO

Paper history:
Received 12 March 2016
Received in revised form 31 July 2016
Accepted 25 August 2016

Keywords:
Ti/TiN/TiCN/TiAlN Coating
Tribology
Cathodic Arc Physical Vapor Deposition
Plasma Assisted Chemical Vapor Deposition
C450 Steel

ABSTRACT

This study investigated the effects of deposition techniques on the microstructural and tribological properties of Ti/TiN/TiCN/TiAlN multilayer coatings onto a Custom 450 steel substrate. The coatings were produced using cathodic arc physical vapor deposition (CAPVD) and plasma-assisted chemical vapor deposition (PACVD). The microstructure of the coatings was evaluated using (SEM), and phase formation was analyzed by (XRD). The mechanical properties of the coatings were examined by nano-indentation testing machine. Erosion behavior was studied using an erosion tester and the electrochemical behavior of the deposited films in 3.5% (wt) NaCl solution was investigated using potentiodynamic polarization. XRD analysis indicated that TiN, TiCN, and TiAlN featured different chemical compositions in each coating. Nano-indentation showed that the hardness of the CAPVD and PACVD coating was 23.35 and 12.92 GPa, respectively. The coefficient of friction was 0.22 for the CAPVD and 0.17 for the PACVD coatings. Erosion testing was conducted using two abrasive powders at impact angles of 30° and 90°. The results showed that erosion rate at an impingement angle of 90° was greater than that of 30° and the CAPVD coating showed better performance. The potentiodynamic polarization curves showed that the CAPVD coating provided better corrosion resistance than the PACVD coating.

doi: *10.5829/idosi.ije.2016.29.10a.17*

1. INTRODUCTION

Custom 450 is a martensitic precipitation hardenable stainless steel used for compressor blades in gas turbines. In aggressive environments, abrasive airborne particles and corrosive agents such as water vapor or salt fog can be ingested into the inlet of a gas turbine and cause premature failure of the blades, which is due to the development of surface pits and transition from pit to crack and propagation of crack due to fatigue loading [1-3]. Use of hard coatings is one of the ways to prevent premature failure. Various coatings have been applied to combat erosion in turbines. Conventional physical vapor deposition (PVD), modified electron beam physical vapor deposition (EB-PVD), and cathode arc physical vapor deposition (CAPVD) are the methods used to deposit these coatings. The most commonly used ones are nitride coatings, including single layered TiN, CrN, and TiCN, TiAlN, TiSiCN, as well as multilayered Cr/CrN and Ti/TiN. Experimental approaches have been used to study the design of TiN-based multilayer coatings to decrease erosion under different erosive conditions for the protection of aerospace components [4, 5]. Thin TiN-based coatings have been applied to gas turbine compressor blades for erosion mitigation with great success [6]. However, based on the engine design, TiN coatings are unsatisfactory for certain operating in desert areas and more erosion resistant coatings are required to improve performance [7, 8]. Immarigeon et al. [9] showed that great differences can be observed for TiN single-layer coatings prepared by different deposition techniques. In their study, thick PVD-deposited coatings were shown

*Corresponding Author's Email: *ak_salarvand@yahoo.com* (A. Salarvand)

Please cite this article as: E. Poursaiedi, A. Salarvand, Comparison of Properties of Ti/TiN/TiCN/TiAlN Film Deposited by Cathodic Arc Physical Vapor and Plasma-assisted Chemical Vapor Deposition on Custom 450 Steel Substrates, International Journal of Engineering (IJE), TRANSACTIONS A: Basics Vol. 29, No. 10, (October 2016) 1459-1468

to have the lowest erosion rate; but, they suggested that poor adhesion might have skewed some of the results. It is known that relatively thick coatings are needed for durable erosion resistance. Also, as the coating thickness increased for the monolayer coatings, the microstructure was changed. A thin coating looked very dense and featureless, while for the thicker coatings, features of V-shaped columnar internal discontinuities appeared [10]. Avila et al. [11] deposited TiN, Ti(C, N), and (Ti,Al)N films through the PAPVD process onto cemented carbide inserts which were used as cutting tools. The highest wear rate, among the coated studied tools was obtained by the TiAlN coated carbide tool. The results of the Rockwell adhesion tests indicated lower adhesion for the (Ti,Al)N system compared to the other systems.

Also, Kwasny et al. [12] obtained Ti + TiN, Ti + TiCxN(1-x), and Ti + TiC PVD coatings on the ASP 30 sintered high-speed steel using magnetron sputtering in the chamber with the controlled temperature. They displayed high micro-hardness, whose value depended on the working atmosphere's composition, temperature in the chamber, and distance of specimens from the magnetron shield. The erosion resistance of the investigated coatings was mostly dependent on the atmosphere composition in the chamber and process temperature.

Antonov et al. [13] assessed the performance of the nano-composite gradient super-hard AlTiN/Si3N4 and also, TiN, TiCN, TiAlN, and AlTiN gradient PVD coatings deposited onto cemented carbide substrate. The relative material performance results arranged the coatings in the row of resistance decrease to wear the studied conditions as follows: nACo -AlTiN-(Gradient) – TiAlN-(Multilayer) – TiCN – TiN, corresponding to the decrease of the hardness of coatings.

Madaoui et al. [14] investigated the corrosion behavior of the TiN and TiCN coatings deposited using magnetron sputtering technique on XC48 steel in a 3.5% NaCl solution. The results unambiguously showed that the coated XC48 steel had better resistance to uniform and pitting corrosion than the bare material and that coating with TiCN further enhanced this performance.

Also, it was found that multilayer coating had better anticorrosion property than monolayer coating [12, 15, 16]. Failures such as pores, crevices, or a columnar structure occurring during single layer deposition can be neutralized by successive deposition of the coating layers. In the latter method, the path of the corrosion agent is either longer or blocked.

Electrochemical testing of a TiN/TiAlN multilayer coating prepared using the reactive DC magnetron sputtering method increased resistance to corrosion caused by 3.5% NaCl solution [15]. The multilayer coating increased the resistance of AISI 1045 steel under corrosion-erosion. The normal impact angle of 90° produced the higher corrosion rates than the impact angle of 30° [16].

Plasma-assisted chemical vapor deposition (PACVD) is a deposition technique to create low-friction coatings. Stoiber et al. [17] developed TiN coatings deposited by PACVD with different chlorine contents to optimize their friction and wear properties, since low-friction coatings with the friction coefficient of 0.17 can be deposited onto three dimensional geometries.

Akbarzadeh et al. [18] studied micro-structural and mechanical properties of TiN, CrN and (Ti,Cr)N coatings applied on tool steel substrates via cathodic arc evaporation method. The highest and lowest levels of hardness were obtained with TiN and CrN coatings, respectively. Also, the (Ti,Cr)N coating provided the highest Young's Modulus along with the lowest friction coefficient.

Despite the large number of research that has been conducted in the field of hard coatings, few works have been done in the field of gas turbine compressor blade coating and C450 material, in particular for multilayer coating. This study evaluates the microstructure, mechanical properties, erosion and corrosion resistance of Ti/TiN/TiCN/TiAlN multilayer coatings deposited by CAPVD and PACVD onto Custom 450 steel.

2. MATERIAL AND METHODS

2. 1. Sample Preparation Custom 450 stainless steel cut and machined from scrap blades from a gas turbine compressor were used to create samples 3 cm × 3 cm × 0.5 cm in size. The result of chemical analysis of a sample of the material is shown in Table 1. The steel was heated at 1030°C for 0.5 h and was then quenched in water. Precipitation hardening was then carried out at 530°C (1050°F) for 4 h [19] to obtain a microhardness of 310 ± 20 $Hv_{0.3Kgf}$ Prior to deposition, the substrates were ground using 600, 1000, 1500, and 2500 grit size silicon carbide paper and then mirror polished using 1 μm silica suspended in water to obtain a roughness of 0.05 μm.

TABLE 1. Chemical analysis of C450 stainless steel

Element	C	Mn	Si	P	Co	Cr	Ni	Mo	Cu	Nb	V	Fe
Wt%	0.027	0.6	0.245	0.0166	0.0604	15.17	6.43	0.79	1.48	0.35	0.08	Balance

2. 2. Coating Processes

2. 2. 1. Cathode Arc Physical Vapor Deposition (CAPVD) The Ti/TiN/TiCN/TiAlN coating was deposited using CAPVD method. The deposition chamber was a cylindrical stainless steel rector 800 mm in diameter and 500 mm in height. The samples were mounted in holders in a planetary system around a circular plate. Argon with purity of 99.99% was used for cleaning. The reactive gas was nitrogen (99.99% purity) and used for the coating layers.

A Ti target (99.99% purity) and TiAl target (70%-30%) were used for the Ti/TiN/TiCN/TiAlN coating. Table 2 lists the process parameters for the coatings.

2. 2. 2. Plasma-assisted Chemical Vapor Deposition (PACVD) Ti/TiN/TiCN/TiAlN multilayer coating was deposited onto C450 substrate by PACVD using pulsed DC current (10 kHz). The samples were washed with acetone in an ultrasonic bath for 3 min. The surface samples were then cleaned by spattering under argon and hydrogen plasma gas flow at 6 amps for 1 h. For the deposition of titanium (buffer layer), the titanium tetrachloride vapor entering the chamber was cut with nitrogen gas.

$$TiCl_4+2H_2 \rightarrow Ti+4HCl \quad (1)$$

For deposition of TiN, nitrogen gas entered the plasma environment at a flow rate of $40 cm^3.min^{-1}$; to create the TiCN layer, methane gas (CH_4) at a flow rate of 5 $cm^3.min^{-1}$ entered as in the previous phase. For deposition of the TiAlN layer, the methane gas flow was stopped and the aluminum tetra chloride vapor entered chamber; the layer was created as follows:

$$2AlCl_3+3H_2 \rightarrow 2Al+6HCl \quad (2)$$

Table 3 lists the condition parameter of PACVD. The ideal temperature for this process is 530°C [17, 20], but a substrate temperature of 470°C was used to avoid exceeding the aging temperature of the martensitic precipitation hardenable stainless steel.

TABLE 2. Process parameters for PVD coatings

Coating parameters	Ti/TiN/TiCN/TiAlN
Target	Ti (99.999% and TiAl (70%-30%)
Inert gas	Ar
Reactive gas	N_2, CH_4
Bias voltage	50V
Deposition temperature	300°C
Deposition rate	40 $nm.min^{-1}$
Vacuum chamber pressure	26.6×10^{-6} bar
Bond coat	Ti
Current	95A(Ti), 90A(TiAl)

TABLE 3. Process parameters for PACVD

Coating parameters	Values			
Discharge voltage	550-600V			
Pulse duration (f)	8 kHZ			
Temperature	450°C			
Duty cycle	33%			
Pressure of chamber	1 bar			
Gases flow rate ($cm^3.min^{-1}$) in layers				
Gases	Ti	TiN	TiCN	TiAlN
Ar	75	75	75	75
N_2	250	250	250	250
H_2	0	40	40	40
CH_4	0	0	5	0
$TiCl_4$	3	3	3	3
$AlCl_4$	0	0	0	2

2. 3. Analytical Methods

2. 3. 1. Scanning Electron Microscope FE-SEM (TESCAN MIRA3 LMU and ZEISS) was used to observe microstructure, the surface topography and cross-sections of all coatings.

2. 3. 2. X-Ray Diffraction (XRD) Analysis An X-ray diffraction (XRD) (Philips) was employed to investigate the crystal structures of the coating processes by the θ-2θ method on the coating surface. A Cu K_αX-ray source with a wavelength (λ) of 0.154 nm was utilized, and scan ranges (2θ) were set from 4° to 90°.

The X-ray peak identifications and lattice parameter calculations were conducted with an X'pert high score software package (Materials Data, Inc).

2. 3. 3. Nano-indentation The mechanical properties including hardness (H), modulus of elasticity (E) and coefficient of friction of the thin coatings were measured using a nano-indentation tester (Hystron).

2. 4. Erosion Test Erosion tests were designed based on ASTM G 76-07standard [20]. The abrasive particles were dispersed by controlling the feed rate of powder and the speed of flow. The airflow was controlled and monitored using a pressure gage and also with the help of a Rotameter (Figure 1). The key parameters are summarized in Table 4. Silica powders (SiO_2) with two different particle size distributions, were chosen as erodent that their characteristics are summarized in Table 5. A feed rate of 2 $g.min^{-1}$ was used for all of the erosion tests. The impingement angles of 30° and 90° were used at the speeds of 100 and 160 $m.s^{-1}$. Table 6 lists the design parameters of the tests.

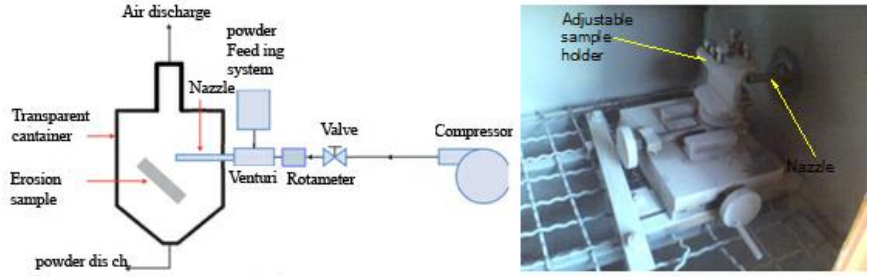

Figure 1. Schematic sketch and internal view of erosion tester

TABLE 4. Key parameters of the erosion test

Parameters of the testing	Value
Carrier fluid	Air under room conditions (1 bar, 24°C)
Line pressure	6 bar
Sand feed rate	2 g. min^{-1}
Test duration	17 min
Nozzle ID	4 mm
Nozzle length	100 mm
Nozzle-coupon distance	10 mm

TABLE 5. Specification of erodent

Erodent type	Erodent material	D_{97}	D_{50}
1	Silica (SiO_2)	40µm	17µm
2	Silica (SiO_2)	12µm	7µm

TABLE 6. Erosion test parameters

Erodent	Velocity of particles ($m.s^{-1}$)	Impingement angle(deg)
Type 1	100	30
Type1	100	90

All of the tests were performed on both uncoated and coated samples. Each test lasted 17 min. To determine the mass loss of each sample, samples were weighed prior to the test and after 2,7, and 17 min from the onset of the test using a scale with the readability of five decimal places to the right of the decimal point (0.0000lg). To avoid the removal of the entire coating, after every two minutes, the impact place of the particles was displaced for a centimeter so that the whole surface of the sample with a total area of 9 square centimeters to be covered.

2. 5. Corrosion Test The electrochemical behavior of the TiN/TiCN/TiAlN coatings on C450 steel in a NaCl 3.5% solution was studied using an Electro-analyzer (SAMA500) potentiostat controlled by the Sama software. Prior to each measurement, the sample was exposed to corrosion test at open circuit potential in the corrosion test solution for 3h to ensure the stabilization potential. All experiments were conducted at constant temperature of 25 ℃.

The polarization curves were plotted by scanning the electrode potentials at $5mV.s^{-1}$. A saturated calomel electrode (SCE) was used as reference (to measure the potential across the electrochemical interface) and a platinum sheet as counter electrode. Data were automatically collected and analyzed using Sama Software.

3. RESULTS AND DISCUSSION

3. 1. Microstructural and Chemical Compositions of the Coatings Figures 2 and 3 show the cross-sectional and surface views of the coatings. Figure 2(a) shows that the CAPVD coatings adhered fairly well to the substrate. The thickness of the buffer layer (Ti) was low (200 nm). The TiN layer had a columnar structure with a thickness of about 0.8 µm. The TiCN layer had a crystalline structure with very fine grains, relatively low porosity, and a layer thickness of about 0.7 µm. The TiAlN layer fully adhered to the bottom layer and had very fine grains and a thickness of about 0.9 µm. Figure 2(b) is a surface view of the CAPVD coating. SEM observations showed that the growth mechanism in this coating was layer by layer.

Figures 3(a) and 3(b) are a cross-section and a surface view of the Ti/TiN/TiCN/TiAlN coating applied by PACVD, respectively. The SEM micrograph of the cross-section clearly shows that the PACVD coating is free of columnar structure. The close-up of the surface shows a cauliflower-like pattern (Figure 3(b)) that does not appear to be the result of crystallization by epitaxial growth, which is typical of many coatings. The cross-section of the coating (Figure 3(a)) shows that the film layers had thicknesses of 0.6, 0.9, and 0.8 µm for the TiN, TiCN, and TiAlN, respectively. The bond layer was about 100 nm in thickness. The substrate-film interface for the PACVD coating appears to be slightly rough with micro-cracks that caused slightly weaker

adhesion to the substrate. SEM images of the PACVD coating surface indicated an island growth mechanism on a scale of 100 nm, with each island composed of smaller islands.

In general, the CAPVD coating had a rougher surface than the PACVD coating because cathodic arc deposition usually generates large amounts of droplets during deposition. The defects of the CAPVD coating included nodules and nodule-detached craters associated with the formation of droplets and pinholes created by the impact of macroparticles on the surface, which typically generates a rough surface. All analysis was done using a scattered electron detector and, at times, a back-scattered electron detector.

Figures 4(a) and 4(b) shows typical XRD patterns of Ti/TiN/TiCN/TiAlN multilayer coating by PACVD and CAPVD, respectively. Analysis of the XRD results identified the compounds as having the chemical formulas TiN, $TiC_{0.2}N_{0.8}$, $TiC_{0.51}N_{0.12}$, Ti_3AlN, and $Ti_3Al_2N_2$ with orientation planes of (1 1 1), (2 0 0), (2 2 0), (3 1 1), and (2 2 2) in both types of coating. Since the thickness of coatings is less than 5µm, some peaks corresponding to the substrate (such as Ni-Cr-Fe and Fe_3C) can be detected which were previously ignored.

NaCl-type crystals of crystalline TiN were observed at (35.97°), (41.76°), and (60.57°) with d-spacing and orientation planes of 2.49 (1 1 1), 2.16 (2 0 0), and 15.2 (2 2 0), respectively. Dissolution of C and Al atoms into the TiN lattice and creation of the $TiC_{0.2}N_{0.8}$ and Ti_3AlN phases caused the patterns peaks to shift and the d-spacing to decrease. For example, for $TiC_{0.2}N_{0.8}$, these were 2.45 (1 1 1), 2.12 (2 0 0), and 1.50(2 2 0) and for Ti_3AlN were 2.37 (1 1 1), 2.05 (2 0 0), and 1.45 (2 2 0). The crystal lattice was hexagonal for $Ti_3Al_2N_2$ with the preferred orientation plane and d-spacing of 11.67 (0 0 2) and for $TiC_{0.51}N_{0.12}$ at 2.15 (0 1 4). Also, such compounds as AlN and TiC were found in the XRD pattern of the CAPVD coating. Evaluation of the XRD pattern for the PACVD coating found the presence of chlorine. The presence of these different compounds represents reason explaining the difference in the picks along the two patterns. The trace element of chlorine could have been introduced by $TiCl_4$ and $AlCl_4$ vapor during deposition. The retained Cl_2,$TiCl_4$ and $AlCl_4$ could have become entrapped in the pores [21], at the grain boundaries, or been associated with other micro-defects in the coatings. The chlorine content was expected to be harmful to hardness and erosion and corrosion resistance [22], but, on the contrary, it can contribute to lowering of the friction coefficient of the PACVD coatings [23].

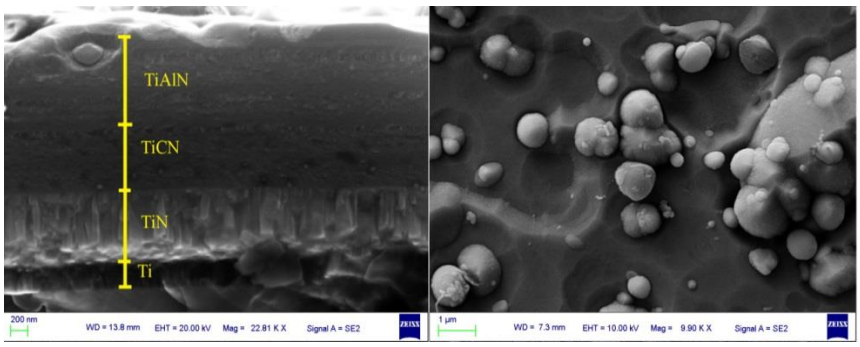

Figure 2. SEM of Ti/TiN/TiCN/TiAlN coating by CAPVD: (a) cross-section and (b) surface view

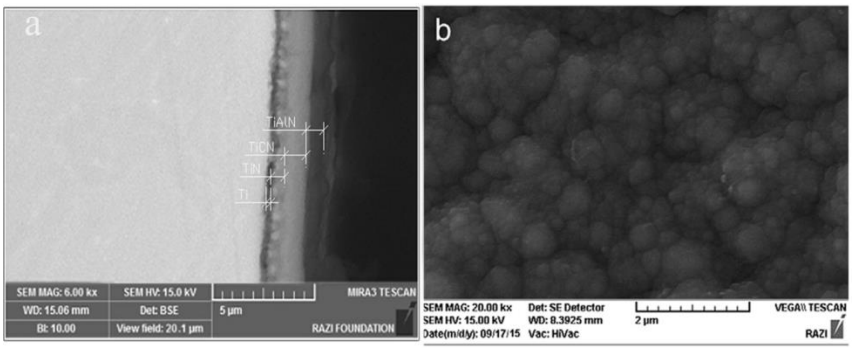

Figure 3. SEM of Ti/TiN/TiCN/TiAlN coating by PACVD: (a) cross-section and (b) surface view

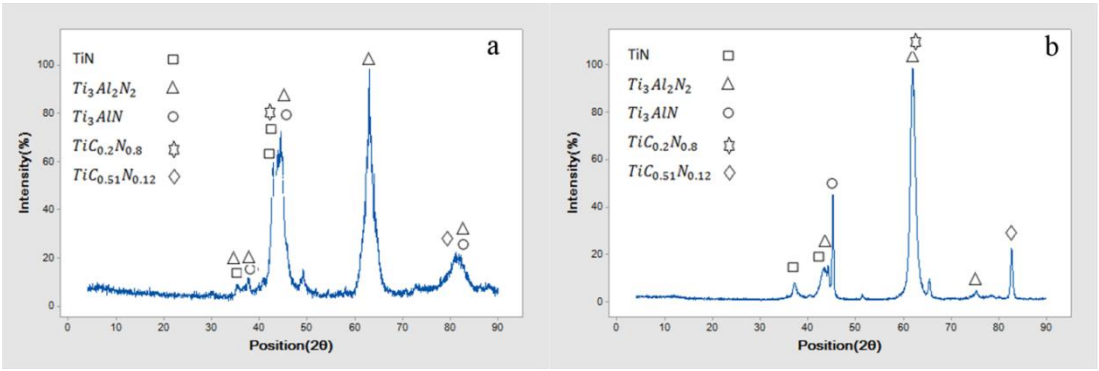

Figure 4. XRD patterns of the multilayer Ti/TiN/TiCN/TiAlN coating by (a) PACVD and (b) CAPVD

3. 2. Mechanical Properties The hardness of the coatings was evaluated using a nano-indenter (Hystron) with a Berkovich diamond indenter. The instrument applied a maximum load of 10mN. To compensate for possible non-uniformity of the coatings, a total of 7 indents were performed and the results were averaged (Table 7).

The values obtained for nanohardness and elastic modules are given in Table 7 and were in good agreement with the values found elsewhere [16, 24]. The results showed that, the CAPVD coating had higher hardness and modulus of elasticity than the PACVD coating. The layer-by-layer growth mechanism seems to be the main cause of such an increase in modulus of elasticity.

A recent study has demonstrated the correlation between the H/E ratio and erosion rate. Because the volume of plastic deformation generated during an indentation is inversely proportional to H/E [25], the erosion rate should decrease as the H/E increases. The results in Table 7 show that the CAPVD coating recorded the highest H/E. Also $\frac{H^3}{E^2}$ ratio is an indication of higher resistances to plastic deformation [26, 27].

3. 2. 1. Coefficient of Friction Nano-scratch tests with normal and lateral forces onto the surface of each sample were conducted (Figure 5). For PACVD coating maximum normal force was 9941 and 1625μN in lateral and also for CAPVD maximum normal force was 9965 and 2156μN in lateral. Figures 5(a) and 5(b) indicate that the coatings showed good adhesion to the substrate without delamination after applied loading. The coefficient of friction as the ratio of lateral to normal force was determined and the amount of 0.17 and 0.22 for PACVD and CAPVD coatings was obtained, respectively. These results can be deduced from the graphs in Figure 6. The jump in Figure 6(b) could be the result of subduction caused by changes in the vertical displacement of the indenter. Surface roughness can affect coefficient of friction in the CAPVD coating.

3. 3. Erosion Performance Erosion was dependent on the density of the film, its hardness, and adhesion to the substrate. The erosion rate for hard coatings is expressed as weight loss per unit of erodent.

TABLE 7. Average nano-indentation parameters

Parameters	Depth of indent (nm)	Force (μN)	H(Berk. Hardness) (GPa)	E (Module of elasticity) (GPa)	H/E (GPa)	H^3/E^2
Ti/TiN/TiCN/TiAlN (CAPVD)	165.	9942.3	23.35	269.05	0.0867	0.1758
Ti/TiN/TiCN/TiAlN (PACVD)	198.9	9936	12.92	227	0.0569	0.0418

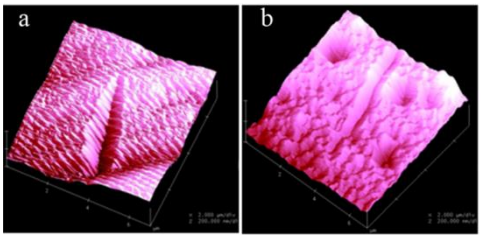

Figure 5. AFM images of the scratch test: (a) PACVD coating and (b) CAPVD coating surface

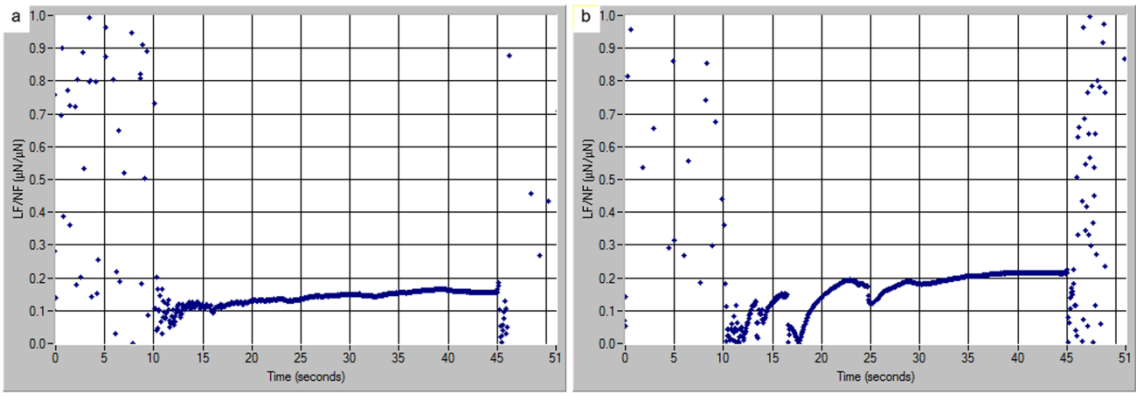

Figure 6. Determination of the coefficient of friction on the nano-scratch test: (a) PACVD coating and (b) CAPVD coating

Figure 7(a) shows erosion testing using a 30° impingement angle, velocity of 100 $m.s^{-1}$ and article diameter of 12µm. Figures 7(b), (c) and (d) plot the mass loss of samples versus erodent mass for the other states. The erosion rate of CAPVD coating at both impingement angles, are significantly lower than PACVD coatings due to its higher hardness and Young's modulus. The erosion rate for both the CAPVD and the PACVD coating increased with increases of impingement angle; this is an indication of a brittle erosion mode. Also, the erosion rate for both types of coating is less than uncoated material. The erosion rates, versus mass loss per unit of erodent for different conditions are summarized in Table 8.

3. 4. Corrosion Performance The polarization curves of bare and coated C450 in 3.5% NaCl solution, after stabilization period of the open circuit potential, are shown in Figure 8. The parameters are listed in Table 9. The polarization resistance R_p and the corrosion rate (corrosion current) are important kinetic parameters that can characterize the corrosion behavior of a material. A high R_p denotes low corrosion rate (corrosion current). It is shown from Table 9 and Figure 8 that both PACVD and CAPVD coatings exhibit different corrosion behaviors. In the case of CAPVD coating, the corrosion potential is more positive than PACVD coating which could be traced back to its denser microstructure.

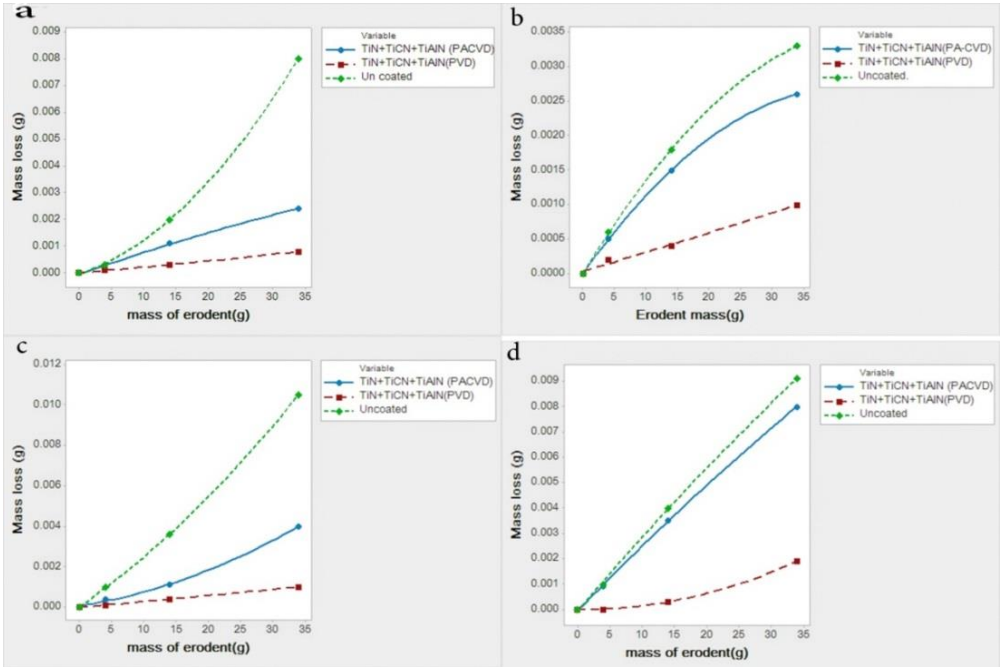

Figure 7. Mass loss versus erodent mass exposure for coated and uncoated materials at: particle velocity (V); particle size (D) and impingement angle (A) of : (a) V= 100 $m.s^{-1}$; D= 12 µm; A= 30°, (b) V= 100 $m.s^{-1}$; D= 12 µm; A= 90°, (c) V=160 $m.s^{-1}$; D= 40 µm; A= 30° and (d) V=160 $m.s^{-1}$; D= 40 µm; A= 90°.

Moreover, the ratio of the corrosion rate of CAPVD coating to that of PACVD coating is 2.1 (Table 8). The more positive potential of CAPVD coating and its lower corrosion rate express a better resistance to uniform and pitting corrosion. The weaker performance of PACVD coating could be due to larger grain size and so existence of chlorine gas at boundaries of grains that caused diffusion of corrosive materials into the coating film. Also, the island structure and close inter-grain distances in this coating can contribute to intergranular corrosion. This resistance can be enhanced via the optimization of the deposition process parameters such as temperature and the composition of gas mixture [17].

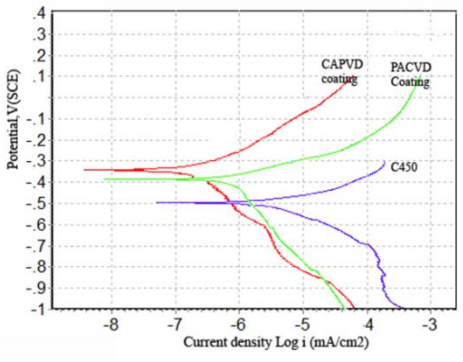

Figure 8. Polarization curves of C450, C450 + CAPVD coating and C450 + PACVD coatings in 3.5% NaCl solution

TABLE 9. Electrochemical parameters (corrosion potential (E_{corr}), corrosion current (i_{corr}), anodic Tafel slope (Ba), cathodic Tafel slope (Bc) and polarization resistance (R_p) of C450, PACVD and CAPVD coating in 3.5% NaCl solution.

Material	i_{corr} ($\mu A.cm^{-2}$)	R_p ($ohm.cm^2$)	E_{corr} (V)	(Ba) (V/dec)	(Bc) (V/dec)
C450	440	637.3	-0.496	1.083	1.55
PACVD coated	71.2	4685.6	-0.352	1.21	2.02
CAPVD coated	33.8	10644	-0.34	1.441	1.95

4. CONCLUSION

The present study evaluated the characterizations of Ti/TiN/TiCN/TiAlN multilayer coating deposited using PACVD and CAPVD techniques. The results indicated that deposition process was a major factor governing the microstructure and mechanical properties of the coating system. Microstructural analysis of the coatings showed that the coating deposited by CAPVD method had better density, toughness, and adhesion than PACVD coating. However, it was not a good surface quality. Also, nano-indentation tests showed that CAPVD coating had hardness, elastic modulus, and ratio of $\frac{H^3}{E^2}$ compared to PACVD coating. Therefore, the plastic deformation is lower and erosion resistance is higher. Another result is that both coatings had a brittle nature, which could be significant for CAPVD coating. Electrochemical corrosion tests showed that CAPVD coating had better performance, which was due to having denser structure and very fine grains. The major results are the following:

- The coefficient of friction of the final surfaces was 0.22 for the CAPVD coating and 0.17 for the PACVD coating.
- The hardness of the CAPVD and PACVD coating was 23.35 and 12.92 GPa, respectively.
- The samples subjected to erosion testing showed that the rate of erosion for the PACVD coating was 3- to 4.7-fold that of the CAPVD coating.
- The corrosion rate of the CAPVD and PACVD coating was 33.8 and 71.2 ($\mu A.cm^{-2}$), respectively.

It was concluded that the CAPVD coating can be improved by increasing the quality of its surface. The PACVD coating could be improved by selecting the appropriate process parameters and the amount of free chlorine in the coating, which should be minimized as much as possible to avoid decreasing the values of the mechanical properties. There are evident limits for increasing the temperature of the process.

5. ACKNOWLEDGMENTS

The authors would like to thank the South Pars Gas Company (SPGC) for the financial support of the project.
Thanks to managers and engineers of the company for their helps during the project.

6. REFERENCES

1. Poursaeidi, E., Babaei, A., Behrouzshad, F. and Arhani, M.M., "Failure analysis of an axial compressor first row rotating blades", ***Engineering Failure Analysis***, Vol. 28, (2013), 25-33.
2. Hamed, A., Tabakoff, W. and Wenglarz, R., "Erosion and deposition in turbomachinery", ***Journal of Propulsion and Power***, Vol. 22, No. 2, (2006), 350-360.

3. Linden, D., "Long term operating experience with corrosion control in industrial axial flow compressors", in Proceedings of 14th Turbomachinery Symposium., (2011), 12-15.
4. Borawski, B., Todd, J.A., Singh, J. and Wolfe, D.E., "The influence of ductile interlayer material on the particle erosion resistance of multilayered tin based coatings", ***Wear***, Vol. 271, No. 11, (2011), 2890-2898.
5. Borawski, B., "Multilayer erosion resistant coatings for the protection of aerospace components", (2011).
6. Bielawski, M. and Beres, W., "FE modelling of surface stresses in erosion-resistant coatings under single particle impact", ***Wear***, Vol. 262, No. 1, (2007), 167-175.
7. Yang, Q., Seo, D., Zhao, L. and Zeng, X., " Erosion resistance performance of magnetron sputtering deposited TiAlN coatings", ***Surface and Coatings Technology***, Vol. 188, (2004), 168-173.
8. Swadzba, L., Maciejny, A., Formanek, B., Liberski, P., Podolski, P., Mendala, B., Gabriel, H. and Poznanska, A., "Influence of coatings obtained by pvd on the properties of aircraft compressor blades", ***Surface and Coatings Technology***, Vol. 78, No. 1, (1996), 137-143.
9. Immarigeon, J.-P., Chow, D., Parameswaran, V., Au, P., Saari, H. and Koul, A.K., "Erosion testing of coatings for aero engine compressor components", ***Advanced Performance Materials***, Vol. 4, No. 4, (1997), 371-388.
10. Swminathan, V., Wei, R. and Gandy, D.W., "Erosion resistant nano technology coatings for gas turbine components", in ASME Turbo Expo 2007: Power for Land, Sea, and Air, American Society of Mechanical Engineers., (2007), 7-16.
11. Avila, R., Godoy, C., Abrao, A. and Lima, M., " Topographic analysis of the crater wear on TiN, Ti(C, N) and (Ti,Al)N coated carbide tools ", ***Wear***, Vol. 265, No. 1, (2008), 49-56.
12. Kwasny, W., Dobrzanski, L. and Bugliosi, S., " Ti + TiN, Ti + Ti (CxN1−x), Ti + TiC PVD coatings on the ASP 30 sintered high-speed steel", ***Journal of Materials Processing Technology***, Vol. 157, (2004), 370-379.
13. Antonov, M., Hussainova, I., Sergejev, F., Kulu, P. and Gregor, A., "Assessment of gradient and nanogradient pvd coatings behaviour under erosive, abrasive and impact wear conditions", ***Wear***, Vol. 267, No. 5, (2009), 898-906.
14. Madaoui, N., Saoula, N., Zaid, B., Saidi, D. and Ahmed, A.S., "Structural mechanical and electrochemical comparison of TiN and TiCN coatings on XC48 steel substrates in NaCl 3.5% water solution", ***Applied Surface Science***, Vol. 312, (2014), 134-138.
15. Ananthakumar, R., Subramanian, B., Kobayashi, A. and Jayachandran, M., "Electrochemical corrosion and materials properties of reactively sputtered TiN/TiAlN multilayer coatings", ***Ceramics International***, Vol. 38, No. 1, (2012), 477-485.
16. Caicedo, J., Cabrera, G., Aperador, W., Escobar, C. and Amaya, C., " Corrosion-Erosion Effect on TiN / TiAlN Multilayer", ***Journal of Materials Engineering and Performance***, Vol. 21, No. 9, (2012), 1949-1955.
17. Stoiber, M., Badisch, E., Lugmair, C. and Mitterer, C., "Low-friction tin coatings deposited by PACVD", ***Surface and Coatings Technology***, Vol. 163, (2003), 451-456.
18. Akbarzadeh, M., Shafyei, A. and Salimijazi, H., " Characterization of TiN, CrN and (Ti, Cr) N Coatings Deposited by Cathodic ARC Evaporation ", ***International Journal of Engineering Transaction A***, Vol. 27, (2014), 1127-1132.
19. T.Kosa, T.A.DeBold., **ASTM STP672,** American Society for Testing and materials, (1979), 367-381.
20. Raoufi, M., Mirdamadi, S., Mahboubi, F., Ahangarani, S., Mahdipoor, M. and Elmkhah, H., "Correlation between the surface characteristics and the duty cycle for the PACVD-derived TiN nanostructured films", ***Surface and Coatings Technology***, Vol. 205, No. 21, (2011), 4980-4984.
21. Dorfel, I., Osterle, W., Urban, I., Bouzy, E. and Morlok, O., "Microstructural characterization of binary and ternary hard coating systems for wear protection Part II: Ti(CN) PACVD coatings", ***Surface and Coatings Technology***, Vol. 116, (1999), 898-905.
22. He, Y., Apachitei, I., Zhou, J., Walstock, T. and Duszczyk, J., "Effect of prior plasma nitriding applied to a hot-work tool steel on the scratch-resistant properties of PACVD TiBN and TiCN coatings", ***Surface and Coatings Technology***, Vol. 201, No. 6, (2006), 2534-2539.
23. Badisch, E., Stoiber, M., Fontalvo, G. and Mitterer, C., " Low-friction PACVD TiN coatings: influence of Cl-content and testing conditions on the tribological behavior ", ***Surface and Coatings Technology***, Vol. 174, (2003), 450-454.
24. Shafiei, S.M.M., Divandari, M., Boutorabi, S.M.A. and Naghizadeh, R., "Comparison of properties TiN/TiCN plasma nitriding films deposited on the tool steel by pulsed dc-PACVD", ***Iranian Journal of Material Science & Engineering***, Vol. 12, No. 2, (2015), 47-55.
25. Chen, J. and Bull, S., "A critical examination of the relationship between plastic deformation zone size and young's modulus to hardness ratio in indentation testing", ***Journal of Materials Research***, Vol. 21, No. 10, (2006), 2617-2627.
26. Tsui, T.Y., Pharr, G.M., Oliver, W.C., Bhatia, C.S., White, R.L., Anders, S., Anders, A. and Brown, I.G., "Nano-indentation and nano-scratching of hard coatings for magnetic disks", ***Material Research Sociaty***, Vol. 383, (1995), 447-452.
27. Musil, J., Kunc, F., Zeman, H. and Polakova, H., "Relationships between hardness, young's modulus and elastic recovery in hard nanocomposite coatings", ***Surface and Coatings Technology***, Vol. 154, No. 2, (2002), 304-313.

Comparison of Properties of Ti/TiN/TiCN/TiAlN Film Deposited by Cathodic Arc Physical Vapor and Plasma-assisted Chemical Vapor Deposition on Custom 450 Steel Substrates

E. Poursaiedi, A. Salarvand

Department of Mechanical Engineering, University of Zanjan, Zanjan, Iran

P A P E R I N F O

Paper history:
Received 12 March 2016
Received in revised form 31 July 2016
Accepted 25 August 2016

Keywords:
Ti/TiN/TiCN/TiAlN Coating
Tribology
Cathodic Arc Physical Vapor Deposition
Plasma Assisted Chemical Vapor Deposition
C450 Steel

چکیده

در این مطالعه اثرات تکنیک های لایه نشانی بر روی میکرو ساختار و خواص تریبولوژیکی پوششهای چند لایه ای Ti/TiN/TiCN/TiAlN بر روی بستری از فولاد C450 مورد بررسی قرار گرفته است. پوشش با استفاده از روشهای لایه نشانی فیزیکی فاز بخار به کمک قوس (CAPVD) و لایه نشانی شیمیایی فاز بخار به کمک پلاسما (PACVD) ایجاد شد. میکرو ساختار پوششها با استفاده از SEM ارزیابی شد و فازهای شکل گرفته با XRD آنالیز گردید. خواص مکانیکی پوششها بوسیله دستگاه نانو ایندنتیشن آزمایش شد. رفتار فرسایشی با استفاده از یک تستر فرسایش مطالعه شد و رفتار الکترو شیمیایی لایه های رسوب داده شده در محلول ۳/۵ ٪ نمک با استفاده از قطبش پتانسیو دینامیکی مورد بررسی قرار گرفت. آنالیز XRD نشان داد که فازهای TiN، TiCN و TiAlN با ترکیبات مختلف تشخیص داده شده اند. نانو ایندنتیشن نشان دادکه سختی پوششها ۲۳/۳۵ GPa و ۱۲/۹۲ GPa به ترتیب برای پوششهای CAPVD و PACVD بود. ضریب اصطکاک برای پوشش CAPVD برابر ۰/۲۲ و ۰/۱۷ برای پوشش PACVD بود. تست سایش با دو پودر ساینده در زوایای برخورد ۳۰° و ۹۰° انجام شد. نتایج نشان داد که نرخ فرسایش در زاویه برخورد ۹۰° بزرگتر از ۳۰° بود وپوشش CAPVD عملکرد بهتری داشت. منحنی های قطبش پتانسیودینامیکی نشان داد که پوشش CAPVD مقاومت به خوردگی بهتری را نسبت به پوشش PACVD فراهم آورد

***doi**: 10.5829/idosi.ije.2016.29.10a.17*